Development of earthquake scenarios for use in earthquake risk analysis for lifeline systems

Yajie J. Lee[1] and William P. Graf[1]

[1]URS Corporation, Los Angeles, CA 90017, USA

Email: Jerry_Lee@urscorp.com, William_Graf@urscorp.com

ABSTRACT

In the most common probabilistic approach to multi-site seismic risk assessment, system response (losses, downtime, etc.) are computed for a comprehensive set of earthquake simulations (or scenarios), referred to here as an 'event set', to account for the potential risks from earthquakes in a region. Detailed models of large lifeline systems are often quite complex, so it may not be practical (or even possible) to analyze the system in detail for an exhaustive set of earthquake scenarios. This paper presents an improved methodology based on Chang et al. (2000) that better incorporates the ground motion uncertainty in the process of selecting a reduced set of hazard-consistent scenarios, and demonstrates its application to the Los Angeles Department of Water and Power network systems.

KEYWORDS: Lifeline, Network system, Earthquake, Risks

1. INTRODUCTION

Seismic risk analysis for a spatially distributed system requires consideration of ground motion correlation to correctly determine the system performance. In the most common probabilistic approach, system response (physical losses, service interruption, etc.) are computed for a comprehensive set of earthquake simulations (or scenarios), referred to here as an 'event set'. Each event or simulation attempts to accurately reproduce the geographic distribution of ground shaking and other hazards from a possible future earthquake. Each event is associated with a frequency of occurrence, where the frequencies are derived from fault activity, magnitude and fault rupture location "sampling". The 'event set' systematically exercises the full range of earthquake magnitudes and rupture locations for each seismic sources, including known faults and background seismicity. The set of scenarios is carefully constructed so that the ensemble accurately reproduces the earthquake hazards' severity and frequency for the region of interest. These simulations usually involve hundreds or perhaps even thousands of scenarios in a complex tectonic region such as southern California, where numerous known and unknown faults exist. Detailed models of large lifeline systems are often quite complex, so it may not be practical to analyze the system in detail for an exhaustive set of earthquake scenarios. As a result, extensive lifeline systems are often analyzed for a reduced set of selected (often maximum) scenarios. A challenge is presented when probabilistic results are needed, since the reduced scenario sample omits many events and their associated probabilities.

One approach (Chang et al., 2000) to bridging the probabilistic "gap" between analyzing systems for a full "event set" and analysis of a reduced scenario sample has been to inflate the annual frequencies associated with the scenarios in the reduced set. A new set of event annual frequencies is sought such that the relevant ground shaking hazard computed from the reduced set at the principal sites of interest is made to match a target probabilistic hazard [e.g., the U.S. Geological Survey (USGS) Hazard Mapping Project (Frankel et al, 2002)]. This procedure assumes that when the shaking hazard is made to match, the consequences will match as well, and the resulting risk curves will follow the curves that would result from analysis using the full event set. The procedure works well when system-wide consequences are relatively linear, with vulnerable components concentrated at a few sites (nodes) and found by simply adding independent consequences from site-to-site. However, nonlinearities are introduced by damage thresholds and other features of equipment vulnerability. Furthermore, the redundancy inherent in network systems may allow a system to continue to function with localized damage. Conversely, damage to a single critical

system node in a non-redundant system may disable an extensive network. Components (transmission or distribution pipe lines) linking the sites may be vulnerable, complicating a hazard-based match. Hence a probabilistic approach based on scaling event annual frequencies to match seismic hazards at a few discrete points may not work well for networked lifeline systems. Nevertheless, the method provides a practical way to depict the system risks in a way that is closer to reality than an arbitrarily selected scenario, and provides a more scientifically sound basis when evaluating the effectiveness of competing risk mitigation strategies.

The USGS hazard includes the uncertainty from empirical attenuation models directly in the calculation. In the Chang et. al. 2000 study, the mean hazards that are calculated using the mean attenuation relations from the reduced set of scenarios were optimized to match the USGS full probabilistic hazards. We noticed that while this 'hybrid' approach, which utilizes the mean hazards to match the USGS probabilistic hazards, has the advantage that the attenuation uncertainty is partially considered in the matching process, it suffers from an early ground motion saturation, which is mainly driven by the lack of explicit consideration of ground motion uncertainty. This approach may somewhat underestimate earthquake risks, especially in the range of ground motions that are of significant interest for lifeline systems. Figure 2 directly obtained from Chang et al [2000] study clearly demonstrates this challenge.
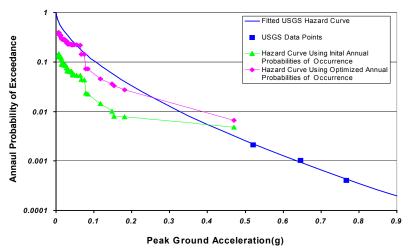

Figure 1. An example of results from the hazard matching process (Reproduced from Chang, Shinozuka and Morre, Presentation, 2000)

We can see from Figure 1 that the USGS ground motion at 2475-year return period reaches about 0.77g, while the maximum ground motion calculated using the mean attenuation relations from the selected scenarios reaches only about 0.46g. It is possible to consider the ground motion uncertainty afterwards in the risk analysis. However, this could lead to the double counting of attenuation uncertainty, which tend to overestimate system risks.

This paper presents an improved method in which the ground motion attenuation uncertainties are included in the process of assigning the frequencies to the selected scenarios. The results are used for the risk analysis for the power and water system of the Los Angeles Department of Water and Power (LADWP).

2. GENERAL APPROACH OF HAZARD-MATCHING PROCESS

The ground motion parameters we calculated include the Peak Ground Acceleration (PGA) and Spectra Acceleration (SA) at 1 second, on a soil condition of NEHRP soil class B/C boundary, as defined in the USGS 2002 hazard maps. PGV, however, is inferred from the spectra responses at 1 second from equation 2.1.

$$PGV = (\frac{981.5}{2\pi} \cdot SA1) \times g / 1.65 \qquad (2.1)$$

where PGV is in unit cm/s, SA1 is the spectral acceleration at 1-second structural period (in units of g), g is the gravity, and the factor of 1.65 in the denominator represents the amplification assumed to exist between peak spectral response and PGV (HAZUS manual, 2005).

Figure 2 shows the locations of target sites that are used for hazard matching (power and water systems, respectively) and the regional faults that are modeled in the USGS 2002 earthquake models.
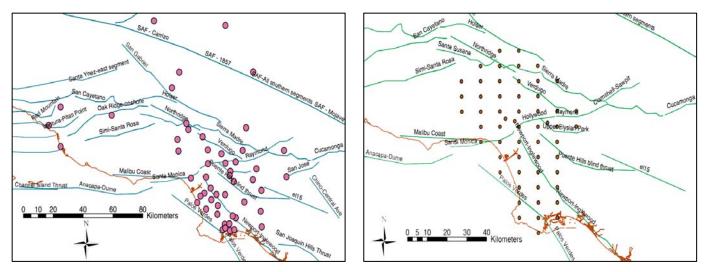

Figure 2. Sites that are used in hazard matching and regional faults (lines). Left: soil circles represent locations of power stations. Right: soil circles represent a grid used for water system.

The USGS 2002 probabilistic hazard calculation includes many kinds of uncertainty. These include the uncertainty in attenuation, uncertainty in fault area vs. magnitude, choice of characteristic vs. Gutenberg-Richter recurrence process, uncertainty in fault limiting magnitude, etc. Model selection (epistemic) uncertainty is accounted for by using a logic tree approach. The randomness (aleatory) uncertainty is accounted for by using either a logic tree approach (for instance, the aleatory fault limiting magnitude uncertainty), systematic randomization (floating events along explicit faults), or statistical distributions may be included directly (for instance, the ground motion attenuation prediction uncertainty from attenuation relations) in the hazard calculation.

To select a candidate set of scenarios for use in the LADWP power and water system risk analysis, we used a relatively large distance interval between floating events along explicit faults, compared to the USGS [Frankel et al]. We estimated the mean values of selected fault parameters (for instance, the limiting magnitude) for use with the candidate scenarios. We further eliminated the logic tree branches for attenuation relations [i.e, Boore et. al. (1997), Sadigh et. al. (1997), Abrahamson and Silver (1997), and Campbell and Bozorgnia (2003)] and calculated the average ground motions from source to site. We then assigned an initial estimate of recurrence frequency to each of our selected scenarios. Since our methodology provides a hazard match though an optimization process that is not sensitive to the starting values, we did not make any effort to achieve an optimal initial frequency estimation. We included the ground motion uncertainty directly into the hazard matching process. Specifically, we adjusted the scenario frequencies so that our calculated probabilistic hazards that include attenuation uncertainty match the USGS hazard values.

Figure 3 shows an example of the results at one target site. We can see from Figure 3 that even though the probabilistic hazard curve matches well with the target, the mean hazard curve can have artificial drop-off. Due to the complexity of the current models in system response analysis, it is difficult to fully adopt the ground motion uncertainty in system response analysis (O'Rouke, 2005; Shinozuka, 2005, personal communication). Therefore, it is desirable to use the mean ground motion attenuation, but with some uncertainty adjustment (a method is proposed later in this paper for this adjustment). To overcome frequency deficiency in the mean hazard curve, we further modified our optimization process to include the misfit of the mean hazard. Specifically, the error function we now minimize includes two parts: one is the misfit between the calculated probabilistic hazards and the target probabilistic hazards, and the other is the misfit between the calculated mean hazards and the target probabilistic hazards. The two errors are summed together with equal weights as our objective error function. With this modification, we are able to control the match for both the mean and the probabilistic hazards. Examples are shown in Figure 4. Other sites show similar good fits.
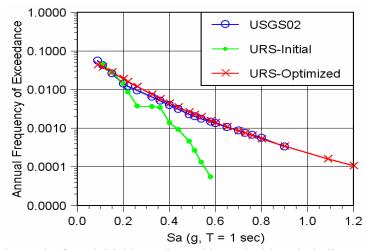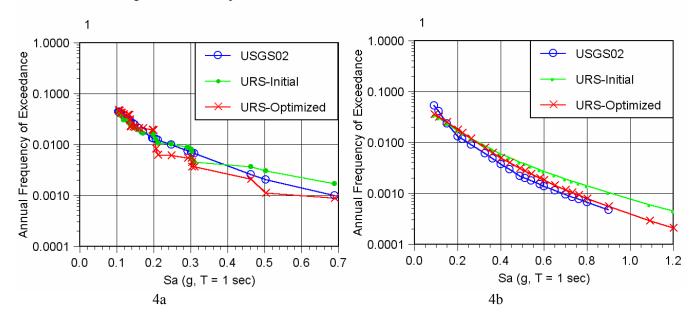

Figure 3. Example results from initial hazard matching. The blue circle line represent the target probabilistic curve. The red cross line represents probabilistic hazard curve calculated from the reduced set of scenarios. The green dot line represents mean hazard curve calculated from the reduced set of scenarios.

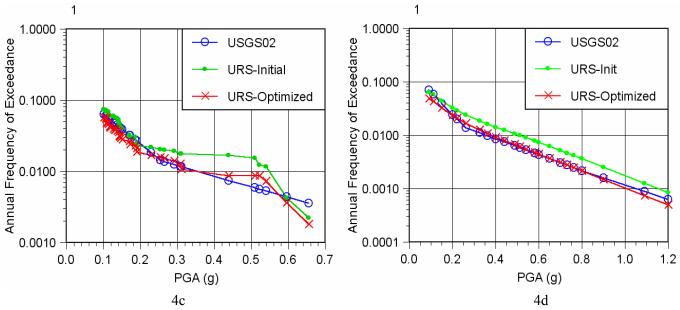4a   4b

Figure 4. An example of hazard matching results. Blue lines are the target hazard at the site. Green lines are hazard curves calculated with our initial assignment of scenario frequencies. Red lines are hazard curves calculated with optimized scenario frequencies. 4a) mean hazard, power system. 4b) probabilistic hazard, power system. 4c) mean hazard, water system. 4d) probabilistic hazard, water system.

3. UNCERTAINTY ADJUSTMENT IN GROUND MOTION PREDICTIONS

The empirical attenuation models are largely constrained by the recordings from historical events. In reality, the number of recordings available from historical events varies drastically. To avoid potential model biases toward events with larger number of recordings, the model parameters are commonly regressed with a two step procedure, in which individual events are weighted equally (Joyner and Boore, 1981; Abrahamson and Youngs, 1992; Abrahamson and Youngs, 1997). As a result, ground motion variations are partitioned into two terms: variation from within the same event (*intra-event* term) and that among different events (*inter-event* term). In essence, the inter-event term accounts for the discrepancy in mean ground motions recorded from earthquake to earthquake, while the intra-event term, on the other hand, measures the randomness of ground motions across a geographic region. In a single-site risk analysis, it makes no material difference in treating them separately. Therefore, the two uncertainties are generally combined and applied as a whole. However, for a spatially distributed system, the implications of the two uncertainty terms are distinct and important. For a uniformly distributed system that consists of a large number of independent system components or risk contributors, the influence of the intra-event variation to the system risk tends to be minimized by redundancy in the system, leading to reduction in the variance of the system response, as system size, complexity and number of components increases. The predicted system loss would approach the expected loss based on the mean ground motion from an event. However, the inter-event variation can bias the predicted system loss systematically higher or lower because of the systematically higher or lower ground motions occurring at all sites from the same event. For a non-uniformly distributed system (for instance, the critical nodes of the network), both terms can be significant to the system risk analysis.

The amount of variability that is attributable to the inter-event and intra-event contribution can vary depending on the attenuation models, the data set used in regression analysis, and the regression method. The following values for the inter-event sigma for the mean ground motion parameters were used:

Table 1. Inter-event uncertainty

Ground Motion Parameter	Inter-event sigma (τ)
PGA	0.31
PGV	0.31
Sa(T=1s)	0.31

These estimates were based on the study (Lee et al., 2000) of the SCEC Phase III project. We averaged the inter-event sigma from Table 3 in Lee et al. 2000 to derive the values. The total variation can be obtained by using a square-root-of-sum-of-the-squares, as $\sqrt{\tau^2 + \sigma^2}$, where τ is the inter-event term, and σ is the intra-event term, which takes a value of 0.5. When mean ground motion attenuation relations are used in system response analysis, it is recommended that one sigma of the inter-event uncertainty term be added to the mean motion throughout the system, to partially compensate for the lack of uncertainty treatment in the model. For the critical nodes in the system, the total uncertainty is recommended for use.

4. RESULTS

4.1. Power system

We used the 52 power substations provided for the LADWP power system as our target sites for selecting the earthquake scenarios and matching the USGS hazards, as shown in Figure 2. We used PGA as the ground motion parameter relevant for hazard matching. To select the candidate scenarios, we used a 0.2g PGA threshold for all stations except Rinaldi and Sylmar, where we retained simulations causing at least 0.1g PGA, based on recommendations. This resulted in a total of 79 earthquake scenarios, of which 72 are from explicit faults and 7 are from background sources. To further reduce the number of scenarios to improve the risk analysis efficiency, we examined the 79 selected scenarios and eliminated those that have minimum contributions to the system risk, for instance, those that generate ground motions above the threshold at less than two substations. Furthermore, we examined the cross correlation of the ground motion patterns for the remaining scenarios and grouped those that have similar magnitude and showed high correlation (with correlation coefficient greater than 0.85). The grouping is based on the assumption that if two simulations with similar magnitudes generate similar ground motion patterns across the system, their system consequences would also be similar. These efforts led to a final of 50 scenarios selected for use with the power system risk analyses, of which 44 are from explicit faults and 6 are from background sources, as listed in Table 2, left panel (attached).

4.2. Water System

We used the 56 grid points for the LADWP water system as our target sites for selecting the earthquake scenarios and matching the USGS hazards. We used spectral acceleration at 1.0 second as the ground motion parameter for hazard matching, as a surrogate for PGV, which is the relevant hazard parameter for the water system. PGV is inferred from SA at 1.0 second, as discussed in Section 2. To select a smaller number of scenarios, we used a threshold of 0.1g SA at 1 second (~10 cm/s PGV) for all grid points. This resulted in a total of 59 earthquake scenarios as listed in Table 3, of which 55 are from explicit faults and 4 are from background sources, as listed in Table 2, right panel (attached).

5. CONCLUSIONS

Earthquake simulations are commonly used for probabilistic risk analysis of geographically distributed systems. These simulations usually involve hundreds or perhaps even thousands of scenarios in a complex tectonic region such as southern California, where numerous known and unknown faults exist. Detailed models of large lifeline systems are often quite complex, so it is not practical to analyze the system for an exhaustive set of earthquake scenarios. As a result, extensive lifeline systems are often analyzed for a reduced set of selected (often maximum) scenarios. In this study, we developed improved approaches to select a reduced set of earthquake scenarios that are based on the models of the USGS 2002 Nation Seismic Hazard Mapping Project, so that the ground motions calculated from these selected scenarios match the USGS ground motions at all facility locations. Due to the importance of ground motion uncertainty in earthquake risk analysis, we considered the uncertainty explicitly in the hazard matching process. Future studies may focus on selecting a reduced set of scenarios and scenario frequencies in order to better match system consequences.

6. ACKNOWLEDGEMENTS

REFERENCES

Abrahamson, N.A., and Silva W.J. (1997). Empirical response spectral attenuation relations for shallow crustal earthquakes: Seismological Research Letters, 68:1, 94-127

Boore, D.M., Joyner, W.B., and Fumal, T.E (1997). Equations for estimating horizontal response spectra and peak acceleration from western North American earthquakes: a summary of recent work, Seismological Research Letters, Vol 68, No. 1, 128-152

Campbell, K.W., and Bozorgnia, Y. (2003). Updated near-source ground motion attenuation relations for the horizontal and vertical components of peak ground acceleration and acceleration response spectra, Bulletin of Seismological Society of America, 93:1, 314-331

Chang, S.E, Shinozuka M., and Moore J.E. (2000). Probabilistic earthquake scenarios: extending risk analysis methodologies to spatially distributed systems, Earthquake Spectra, 16:3, 557-572

Frankel, A.D., Petersen, M.D., Muller, C.S., Haller, K.M., Wheeler, R.L., Leyendecker, E.V., Wesson, R.L., Harmsen, S.C., Cramer, C.H., Perkins, D.M., and Rukstales, K.S. (2002). Documentation for the 2002 Update of the National Seismic Hazard Maps: U.S. Geological Survey, Open-File Report 02-420.

HAZUS Technical Manual (2005). NIBS, 4-10

Lee, Y., Anderson J.G and Zeng, Y. (2000). Evaluation of empirical ground motion relations in southern California, Bulletin of Seismological Society of America, 90:6, Part B, 136-148

Sadigh, K., Chang, C.Y., Egan, J., Makdisi, F., and Youngs, R. (1997). Attenuation relationships for shallow crustal earthquakes based on California strong motion data: Seismological Research Letters, 68, 180-189.

Table 2. Selected scenarios and their optimized recurrence rates. Left: Power system. Right: Water System

Scenario	Recurrence	Magnitude	Scenario Name
12	0.00229783	6.8	Elsinore – Segment 15
18	0.00601694	7.3	San Andreas Fault (SAF) - Mojave
19	0.00148683	7.4	SAF - Carrizo
21	0.00298785	8.1	SAF-All southern segments
22	0.00082355	7.8	SAF - 1857
104	0.00122138	6.4	Hollywood
105	0.00171061	6.5	Raymond
106	0.00129396	6.4	San Jose
138	0.0007867	7.1	Newport-Inglewood
139	0.00148775	6.6	Newport-Inglewood
140	3.54E-05	6.6	Newport-Inglewood
144	0.00109822	7.2	Sierra Madre
145	0.00212262	6.7	Sierra Madre
146	0.00126762	6.7	Sierra Madre
147	0.00196447	7.2	San Gabriel
148	0.00010358	6.7	San Gabriel
151	0.00168977	6.6	Santa Monica
152	0.0012696	6.9	Verdugo
153	5.53E-05	6.4	Verdugo
154	0.00136306	7.2	Mission Ridge-Arroyo Parida-Santa Ana
163	0.00178122	7	Oak Ridge-onshore
165	0.00427163	6.5	Oak Ridge-onshore
166	0.00131423	7	Red Mountain
168	0.00378521	7	San Cayetano
172	0.00152425	6.9	Ventura-Pitas Point
173	0.00067125	6.4	Ventura-Pitas Point
175	0.00292344	7	Simi-Santa Rosa
176	0.00221979	6.5	Simi-Santa Rosa
189	0.00275395	7.5	Anacapa-Dume
190	0.00017366	7	Anacapa-Dume
301	0.00443006	7	Northridge
302	0.00460369	6.5	Northridge
307	0.00010639	7.5	Channel Island Thrust
308	9.40E-05	7	Channel Island Thrust
311	2.66E-06	6.6	Oakridge Mid Channel Mont-Oak
312	0.00100986	7.1	Oakridge-blind thrust offshore
314	0.00127591	6.4	Upper Elysian Park
321	0.00090097	7.1	Puente Hills blind thrust
322	9.72E-05	6.6	Puente Hills blind thrust
336	0.00606367	7.3	Garlock West
354	0.00683535	6.9	Cucamonga
357	0.00116594	7.3	Palos Verdes
359	0.00071548	6.8	Palos Verdes
363	0.00156585	6.3	Palos Verdes
449	0.00158549	6.9	Background Source
450	0.00126876	6.9	Background Source
451	0.00091775	6.9	Background Source
452	0.00081289	6.9	Background Source
453	0.00067956	6.9	Background Source
454	0.0008008	6.9	Background Source

Scennario	Recurrence Rate	Magnitude	Scenario Name
12	0.003598	6.8	Elsinore – Segment 15
18	0.004128	7.3	San Andreas Fault (SAF) - Mojave
19	0.002279	7.4	SAF – Carrizo
21	0.003001	8.1	SAF-All southern segments
22	0.009613	7.8	SAF – 1857
23	0.003365	7.7	SAF – Southern 2 segments
118	0.000166	6.5	Holser
119	6.64E-06	6.4	Hollywood
120	0.000741	6.5	Raymond
122	0.001064	6.5	Clamshell-Sawpit
141	0.002555	7.1	Newport-Inglewood offshore
145	0.001749	7.6	Coronado Bank
159	0.00081	7.1	Newport-Inglewood
160	0.002368	6.6	Newport-Inglewood
161	0.000558	6.6	Newport-Inglewood
162	0.00015	6.6	Newport-Inglewood
166	0.000745	7.2	Sierra Madre
167	0.004398	6.7	Sierra Madre
168	0.000221	6.7	Sierra Madre
169	0.001531	7.2	San Gabriel
170	9.97E-05	6.7	San Gabriel
171	0.001271	6.7	San Gabriel
173	2.70E-06	6.7	Malibu Coast
174	0.000523	6.6	Santa Monica
175	0.000965	6.9	Verdugo
176	1.57E-05	6.4	Verdugo
177	2.84E-06	6.4	Verdugo
189	0.004129	7	Oak Ridge-onshore
191	0.003857	6.5	Oak Ridge-onshore
195	0.006863	7	San Cayetano
196	0.006029	6.5	San Cayetano
198	0.003014	6.7	Santa Susana
202	0.000635	7	Simi-Santa Rosa
203	0.000287	6.5	Simi-Santa Rosa
219	0.000936	7.5	Anacapa-Dume
220	0.00057	7	Anacapa-Dume
221	0.000943	7	Anacapa-Dume
222	1.29E-06	6.5	Anacapa-Dume
370	0.001433	7	Northridge
371	0.000288	6.5	Northridge
372	2.37E-05	6.5	Northridge
378	0.000512	7.5	Channel Island Thrust
388	6.13E-05	6.4	Upper Elysian Park
397	0.000863	7.1	Puente Hills blind thrust
398	1.04E-05	6.6	Puente Hills blind thrust
399	8.21E-05	6.6	Puente Hills blind thrust
440	0.006182	6.9	Cucamonga
443	0.000941	6.7	Sierra Madre-San Fernando
444	0.001051	7.3	Palos Verdes
446	0.00082	6.8	Palos Verdes
447	0.000624	6.8	Palos Verdes
451	0.003275	6.3	Palos Verdes
452	0.001439	6.3	Palos Verdes
453	0.002075	6.3	Palos Verdes
454	0.002167	6.3	Palos Verdes
559	0.001047	7	Background Source
560	0.000775	7	Background Source
561	0.001289	7	Background Source
562	0.000763	7	Background Source